

Diphosphines Possessing Electronically Different Donor Groups: Synthesis and Coordination Chemistry of the Unsymmetrical Di(*N*-pyrrolyl)phosphino-Functionalized dppm Analogue $\text{Ph}_2\text{PCH}_2\text{P}(\text{NC}_4\text{H}_4)_2$

Andrew D. Burrows,^{*,†} Mary F. Mahon,[†] Steven P. Nolan,[‡] and Maurizio Varrone[†]

Department of Chemistry, University of Bath, Claverton Down, Bath BA2 7AY, U.K., and
Department of Chemistry, University of New Orleans, New Orleans, Louisiana 70148

Received May 9, 2003

The unsymmetrical diphosphinomethane ligand $\text{Ph}_2\text{PCH}_2\text{P}(\text{NC}_4\text{H}_4)_2$ **L** has been prepared from the reaction of $\text{Ph}_2\text{PCH}_2\text{Li}$ with $\text{PCl}(\text{NC}_4\text{H}_4)_2$. The diphenylphosphino group can be selectively oxidized with sulfur to give $\text{Ph}_2\text{P}(\text{S})\text{CH}_2\text{P}(\text{NC}_4\text{H}_4)_2$ **1**. The reaction of **L** with $[\text{MCl}_2(\text{cod})]$ ($\text{M} = \text{Pd}, \text{Pt}$) gives the chelate complexes $[\text{MCl}_2(\text{L}-\kappa^2\text{P}, \text{P}')]_2$ (**2**, $\text{M} = \text{Pd}$; **3**, $\text{M} = \text{Pt}$) in which the $\text{M}-\text{P}$ bond to the di(*N*-pyrrolyl)phosphino group is shorter than that to the corresponding diphenylphosphino group. However, the shorter $\text{Pd}-\text{P}$ bond is cleaved on reaction of **2** with an additional 1 equiv of **L** to give $[\text{PdCl}_2(\text{L}-\kappa^1\text{P})_2]$ **4**. Complex **4** reacts with $[\text{PdCl}_2(\text{cod})]$ to regenerate **2**, and with $[\text{Pd}_2(\text{dba})_3]\cdot\text{CHCl}_3$ to give the palladium(I) dimer $[\text{Pd}_2\text{Cl}_2(\mu-\text{L})_2]$ **5**, which exists in solution and the solid state as a 1:1 mixture of head-to-head (HH) and head-to-tail (HT) isomers. The palladium(II) dimer $[\text{Pd}_2\text{Cl}_2(\text{CH}_3)_2(\mu-\text{L})_2]$ **6**, formed by the reaction of $[\text{PdCl}(\text{CH}_3)(\text{cod})]$ with **L**, also exists in solution as a mixture of HH and HT isomers, although in this case the HT isomer prevails at low temperature and crystallizes preferentially. Complex **6** reacts with TIPF_6 to give the A-frame complex $[\text{Pd}_2(\text{CH}_3)_2(\mu-\text{Cl})(\mu-\text{L})_2]\text{PF}_6$ **7**. The reaction of **L** with $[\text{RuCp}^*(\mu_3-\text{Cl})_4]$ leads to the dimer $[\text{Ru}_2\text{Cp}^*2(\mu-\text{Cl})_2(\mu-\text{L})_2]$ **8**, for which the enthalpy of reaction has been measured. The reaction of **L** with $[\text{Rh}(\mu-\text{Cl})(\text{cod})]_2$ gives a mixture of compounds from which the dimer $[\text{Rh}_2(\mu-\text{Cl})(\text{cod})_2(\mu-\text{L})_2]\text{PF}_6$ **9** can be isolated. The crystal structures of **2**· CHCl_3 , **3**· CH_2Cl_2 , **4**, **5**· $1/4\text{CH}_2\text{Cl}_2$, **6**, **7**· $2\text{CH}_2\text{Cl}_2$, **8**, and **9**· CH_2Cl_2 are reported.

Introduction

Diphosphinomethanes such as bis(diphenylphosphino)methane (dppm) are well-established as flexible ligands, with chelating, terminal, and bridging coordination modes all possible.^{1,2} The small bite angle and inherent strain of the chelating mode can lead to interesting chemistry, such as the recent isolation of an alkylrhodium complex stabilized by agostic interactions.³ The reactivities and catalytic properties of diphosphinomethane complexes are dependent on the substituents on the phosphino groups. Thus, for example, palladium(II) complexes of $\text{Ar}_2\text{PCH}_2\text{PAr}_2$, in which Ar is an ortho-substituted phenyl group, are efficient catalysts for

the copolymerization of CO and ethene, in contrast to analogous complexes of dppm.⁴

Unsymmetrical diphosphinomethanes of the general formula $\text{R}_2\text{PCH}_2\text{PR}'_2$ have attracted less attention than their symmetrical analogues. Grim and Mitchell reported ligands of the type $\text{Ph}_2\text{PCH}_2\text{PRR}'$ and studied their group 6 carbonyl derivatives.⁵ More recently Werner et al. have reported the synthesis of a series of unsymmetrical diphosphinomethanes and arsino(phosphino)methanes and presented studies on their coordination chemistry with rhodium^{6,7} and palladium.⁸

We have recently become interested in functionalized *N*-pyrrolyl phosphine ligands, since the *N*-pyrrolyl group

* E-mail: a.d.burrows@bath.ac.uk. Tel: +44 1225 386529. Fax: +44 1225 386231.

[†] University of Bath.

[‡] University of New Orleans.

(1) Puddephatt, R. J. *Chem. Soc. Rev.* **1983**, *12*, 99–127.

(2) Anderson, G. K. *Adv. Organomet. Chem.* **1993**, *35*, 1–39.

(3) Urtel, H.; Meier, C.; Eisenträger, F.; Rominger, F.; Joschek, J. P.; Hofmann, P. *Angew. Chem., Int. Ed.* **2001**, *40*, 781–784.

(4) Dossett, S. J.; Gillon, A.; Orpen, A. G.; Fleming, J. S.; Pringle, P. G.; Wass, D. F.; Jones, M. D. *Chem. Commun.* **2001**, 699–700.

(5) Grim, S. O.; Mitchell, J. D. *Inorg. Chem.* **1977**, *16*, 1770–1776.

(6) Wolf, J.; Manger, M.; Schmidt, U.; Fries, G.; Barth, D.; Weberndörfer, B.; Vicić, D. A.; Jones, W. D.; Werner, H. *J. Chem. Soc., Dalton Trans.* **1999**, 1867–1875.

(7) Werner, H.; Manger, M.; Schmidt, U.; Laubender, M.; Weberndörfer, B. *Organometallics* **1998**, *17*, 2619–2627.

(8) Schmidt, U.; Ilg, K.; Brandt, C. D.; Werner, H. *J. Chem. Soc., Dalton Trans.* **2002**, 2815–2824.

ensures that the phosphorus center is a strong π -acceptor.⁹ As part of this program we have developed the keto-functionalized *N*-pyrrolyl phosphines $\text{Ph}_2\text{P}\{\text{NC}_4\text{H}_3\text{C}(\text{O})\text{Me}-2\}$ ¹⁰ and $(\text{H}_4\text{C}_4\text{N})_2\text{P}\{\text{NC}_4\text{H}_3\text{C}(\text{O})\text{Me}-2\}$ ¹¹ and investigated their properties, including their hemilabile character.¹² In this paper we report the synthesis and group 10 chemistry of the unsymmetrical diphosphinomethane $\text{Ph}_2\text{PCH}_2\text{P}(\text{NC}_4\text{H}_4)_2$, in which the two phosphino groups are isosteric,¹³ but differ strongly in their electronic characters. We also report examples of reactions with ruthenium(II) and rhodium(I) complexes.

Experimental Section

General. Reactions were routinely carried out using Schlenk-line techniques under pure dry dinitrogen or argon, using dry dioxgen-free solvents unless noted otherwise. Microanalyses (C, H, and N) were carried out by Mr. Alan Carver (University of Bath Microanalytical Service). NMR spectra were recorded on JEOL EX-270, Varian Mercury 400, and Bruker Avance 300 spectrometers referenced to TMS or 85% H_3PO_4 . $^{31}\text{P}\{\text{H}\}$ NMR simulations were carried out using gNMR.¹⁴ IR spectra were recorded on a Nicolet Nexus spectrometer as Nujol mulls between KBr disks. The complexes $[\text{PdCl}_2(\text{cod})]$,¹⁵ $[\text{PtCl}_2(\text{cod})]$,¹⁶ $[\text{Pd}_2(\text{dba})_3]\cdot\text{CHCl}_3$,¹⁷ $[\text{PdCl}(\text{CH}_3)(\text{cod})]$,¹⁸ $[\text{RuCP}^*(\mu\text{-Cl})_4]$ ¹⁹ and $[\text{Rh}(\text{cod})(\mu\text{-Cl})_2]$ ²⁰ were prepared by standard literature methods. $\text{Ph}_2\text{PCH}_2\text{Li}$ was prepared according to the method reported by Peterson.²¹ Pyrrole was dried over molecular sieves and distilled before used. Triethylamine was distilled over potassium before use. Calorimetric measurements were made as previously reported.²²

Synthesis of $\text{PCl}(\text{NC}_4\text{H}_4)_2$. A 2.0 M solution of PCl_3 in dichloromethane (72.0 cm^3 , 0.144 mol) was placed in a three-neck flask equipped with a glass frit and a dropping funnel charged with pyrrole (19.34 g, 0.288 mol). The flask was then charged with THF (200 cm^3) and NEt_3 (50 cm^3 , 0.356 mol). The first equivalent of pyrrole was added dropwise over 2 h with stirring, and a white precipitate formed immediately. The reaction mixture was stirred for a further 2 h, and the second equivalent of pyrrole was added dropwise over 4 h. The mixture was stirred overnight and filtered into a Schlenk tube through the frit. The remaining solid was washed with THF, and the washings were combined with the filtrate. The resulting solution was evaporated under reduced pressure to give a

colorless oil. This was kept under reduced pressure (0.2 mbar) at ambient temperature until no more volatiles were present. Distillation (2.0 mbar, 83–85 °C) gave the product as a colorless oil. Yield: 22.6 g (79%). $^{31}\text{P}\{\text{H}\}$ NMR (161.8 MHz, C_6D_6): δ 105.3 (s). ^1H NMR (399.8 MHz, CDCl_3): δ 6.79 (ps quin, 4H, J 2.0 Hz, H_α), 6.18 (ps t, 4H, J 2.0 Hz, H_β). $^{13}\text{C}\{\text{H}\}$ NMR (100.5 MHz, C_6D_6): δ 122.5 (d, $^2J_{\text{CP}}$ 18 Hz, C_α), 113.9 (d, $^3J_{\text{CP}}$ 5 Hz, C_β).

Synthesis of $\text{Ph}_2\text{PCH}_2\text{P}(\text{NC}_4\text{H}_4)_2$ L. A THF solution of $\text{Ph}_2\text{PCH}_2\text{Li}$ (3.46 g, 0.017 mol) was added dropwise with stirring to a THF–hexane solution of $\text{PCl}(\text{NC}_4\text{H}_4)_2$ (3.66 g, 0.018 mol) at –78 °C. The mixture was allowed to reach ambient temperature, stirred for further 2 h, and filtered. Evaporation of the solvent produced a colorless oil, which was triturated with hexane to give a white powder. This was separated by filtration, washed with small amounts of a 1:1 mixture of THF–hexane, and dried under reduced pressure. Yield: 4.62 g (76%). Anal. Calcd for $\text{C}_{21}\text{H}_{20}\text{N}_2\text{P}_2$: C, 69.6; H, 5.56; N, 7.73. Found: C, 69.5; H, 5.58; N, 7.82. $^{31}\text{P}\{\text{H}\}$ NMR (161.8 MHz, CDCl_3): δ 66.1 (d, $^2J_{\text{PP}}$ 147 Hz), –25.5 (d, $^2J_{\text{PP}}$ 147 Hz). ^1H NMR (399.8 MHz, CDCl_3): δ 7.23–7.40 (m, 4H, H_m), 7.37–7.34 (m, 6H, H_o , H_p), 7.00 (ps quin, 4H, H_α), 6.29 (ps t, 4H, H_β), 3.18 (dd, 2H, $^2J_{\text{HP}}$ 6.0 Hz, $^2J_{\text{HP}}$ 1.6 Hz, CH_2). $^{13}\text{C}\{\text{H}\}$ NMR (75.5 MHz, CDCl_3): δ 136.8 (dd, $^1J_{\text{CP}}$ 14 Hz, $^3J_{\text{CP}}$ 8 Hz, C_i), 132.4 (dd, $^2J_{\text{CP}}$ 20 Hz, $^4J_{\text{CP}}$ 2 Hz, C_o), 128.8 (s, C_p), 128.5 (d $^3J_{\text{PC}}$ 7 Hz, C_m), 123.0 (d, $^2J_{\text{CP}}$ 15 Hz, C_α), 112.3 (d, $^3J_{\text{CP}}$ 4 Hz, C_β), 31.0 (dd, $^1J_{\text{CP}}$ 26 Hz, $^1J_{\text{CP}}$ 20 Hz, CH_2).

Synthesis of $\text{Ph}_2\text{P}(\text{S})\text{CH}_2\text{P}(\text{NC}_4\text{H}_4)_2$ 1. Sulfur (0.090 g, 2.81 mmol) was added to a dichloromethane solution of L (0.089 g, 0.25 mmol) and the mixture stirred for 4 h. The undissolved sulfur was removed by filtration, and the solution was concentrated under reduced pressure. On standing for 24 h at –20 °C a yellow crystalline precipitate of sulfur formed which was separated by filtration and discarded. Hexane was added to the filtrate, which on further standing at –20 °C for 24 h gave a colorless solid, which was separated by filtration and dried under reduced pressure. Yield: 0.080 g (82%). Anal. Calcd for $\text{C}_{21}\text{H}_{20}\text{N}_2\text{P}_2\text{S}\cdot\text{CH}_2\text{Cl}_2$: C, 55.1; H, 4.63; N, 5.84. Found: C, 55.1; H, 4.54; N, 6.00. $^{31}\text{P}\{\text{H}\}$ NMR (161.8 MHz, CDCl_3): δ 56.8 (d, $^2J_{\text{PP}}$ 85 Hz), 36.6 (d, $^2J_{\text{PP}}$ 85 Hz). ^1H NMR (399.8 MHz, CDCl_3): δ 7.74–7.68 (m, 4H, H_m), 7.47–7.36 (m, 6H, H_o , H_p), 6.87 (ps quin, 4H, H_α), 6.17 (ps t, 4H, H_β), 3.66 (dd, 2H, $^2J_{\text{HP}}$ 13.2 Hz, $^2J_{\text{HP}}$ 1.2 Hz, CH_2). $^{13}\text{C}\{\text{H}\}$ NMR (75.5 MHz, CDCl_3): δ 131.7 (s), 131.5 (s), 130.7 (d, J 10 Hz), 128.5 (d, J 12 Hz), 123.4 (d, $^2J_{\text{CP}}$ 17 Hz, C_α), 112.3 (d, $^3J_{\text{CP}}$ 3 Hz, C_β), 37.4 (dd, $^1J_{\text{CP}}$ 50 Hz, $^1J_{\text{CP}}$ 26 Hz, CH_2). IR: $\nu(\text{PS})$ 625 cm^{-1} .

Synthesis of $[\text{PdCl}_2(\text{L}-\kappa^2\text{P},\text{P}')] 2$. $[\text{PdCl}_2(\text{cod})]$ (0.155 g, 0.54 mmol) was added to a dichloromethane solution of L (0.197 g, 0.54 mmol). The mixture was stirred for 4 h, and then hexane was added to precipitate a yellow powder. The powder was separated by filtration, washed with hexane, and dried under reduced pressure. Crystallization from dichloromethane–hexane gave yellow crystals. Yield: 0.284 g (97%). Anal. Calcd for $\text{C}_{21}\text{H}_{20}\text{Cl}_2\text{N}_2\text{P}_2\text{Pd}\cdot\frac{3}{4}\text{CH}_2\text{Cl}_2$: C, 43.3; H, 3.59; N, 4.64. Found: C, 43.7; H, 3.60; N, 4.66. $^{31}\text{P}\{\text{H}\}$ NMR (161.8 MHz, CDCl_3): δ 0.0 (d, $^2J_{\text{PP}}$ 84 Hz), –46.7 (d, $^2J_{\text{PP}}$ 84 Hz). ^1H NMR (399.8 MHz, CD_2Cl_2): δ 7.85–7.80 (m, 4H), 7.62–7.57 (m, 2H), 7.51–7.46 (m, 4H), 7.41 (ps quin, 4H, H_α), 6.41–6.40 (m, 4H, H_β), 4.54 (dd, 2H, $^2J_{\text{HP}}$ 12.3 Hz, $^2J_{\text{HP}}$ 10.9 Hz, CH_2).

Synthesis of $[\text{PtCl}_2(\text{L}-\kappa^2\text{P},\text{P}')] 3$. The synthesis was carried out as for compound 2 using $[\text{PtCl}_2(\text{cod})]$ (0.228 g, 0.61 mmol) and L (0.221 g, 0.61 mmol). Crystallization from dichloromethane–hexane gave colorless crystals. Yield: 0.379 g (98%). Anal. Calcd for $\text{C}_{21}\text{H}_{20}\text{Cl}_2\text{N}_2\text{P}_2\text{Pt}\cdot\frac{1}{4}\text{CH}_2\text{Cl}_2$: C, 39.3; H, 3.18; N, 4.31. Found: C, 39.5; H, 3.27; N, 4.49. $^{31}\text{P}\{\text{H}\}$ NMR (121.5 MHz, CD_2Cl_2): δ –16.5 (d, $^2J_{\text{PP}}$ 75 Hz, $^1J_{\text{PPt}}$ 3932 Hz), –57.0 (d, $^2J_{\text{PP}}$ 75 Hz, $^1J_{\text{PPt}}$ 2951 Hz). ^1H NMR (300.2 MHz, CD_2Cl_2): δ 7.86–7.78 (m, 4H),

- (9) Moloy, K. G.; Petersen, J. L. *J. Am. Chem. Soc.* **1995**, *117*, 7696–7710.
 (10) Andrews, C. D.; Burrows, A. D.; Lynam, J. M.; Mahon, M. F.; Palmer, M. T. *New J. Chem.* **2001**, *25*, 824–826.
 (11) Burrows, A. D.; Mahon, M. F.; Palmer, M. T.; Varrone, M. *Inorg. Chem.* **2002**, *41*, 1695–1697.
 (12) Andrews, C. D.; Burrows, A. D.; Jeffery, J. C.; Lynam, J. M.; Mahon, M. F. *J. Organomet. Chem.* **2003**, *665*, 15–22.
 (13) Burrows, A. D. *CrystEngComm* **2001**, *3*, 217–221.
 (14) Budlezaar, P. H. M. *gNMR 4.0*; Cherrwell Scientific Publishing: Oxford, 1997.
 (15) Chatt, J.; Vallarino, L. M.; Venanzi, L. M. *J. Chem. Soc.* **1957**, 3413–3416.
 (16) Drew, D.; Doyle, J. R. *Inorg. Synth.* **1972**, *13*, 47–55.
 (17) Ukai, T.; Kawazura, H.; Ishii, Y.; Bonnet, J. J.; Ibers, J. A. *J. Organomet. Chem.* **1974**, *65*, 253–266.
 (18) Rülke, R. E.; Ernsting, J. M.; Spek, A. L.; Elsevier, C. J.; van Leeuwen, P. W. N. M.; Vrieze, K. *Inorg. Chem.* **1993**, *32*, 5769–5778.
 (19) Fagan, P. J.; Ward, M. D.; Calabrese, J. C. *J. Am. Chem. Soc.* **1989**, *111*, 1698–1719.
 (20) Giordano, G.; Crabtree, R. H. *Inorg. Synth.* **1990**, *28*, 88–90.
 (21) Peterson, D. J. *J. Organomet. Chem.* **1967**, *8*, 199–208.
 (22) Li, C. B.; Serron, S.; Nolan, S. P.; Petersen, J. L. *Organometallics* **1996**, *15*, 4020–4029.

7.58–7.56 (m, 2H), 7.53–7.48 (m, 4H), 7.32 (ps quin, 4H, H_α), 6.42–6.40 (m, 4H, H_β), 4.60 (dd, 2H, ²J_{HP} 13.7 Hz, ²J_{HP} 11.3 Hz, ³J_{HPt} 63.6 Hz, CH₂).

Synthesis of [PdCl₂(L-κ¹P)₂] **4**. Two methods were used:

(a) **L** (0.023 g, 0.063 mmol) was added to a dichloromethane solution of **2** (0.040 g, 0.074 mmol) and the mixture stirred for 30 min. Addition of hexane precipitated out a yellow powder, which was isolated by filtration and dried under reduced pressure.

(b) A dichloromethane solution of [PdCl₂(cod)] (0.102 g, 0.36 mmol) was added dropwise to a stirred dichloromethane solution of **L** (0.259 g, 0.71 mmol) over 2 h. The stirring was continued for an additional 1 h, after which all the solvent was eliminated under reduced pressure. The resulting yellow powder was washed with hexane and dried under reduced pressure. Crystallization from dichloromethane–hexane gave yellow crystals. Yield: 0.313 g (97%). Anal. Calcd for C₄₂H₄₀Cl₂N₄P₄Pd: C, 55.9; H, 4.47; N, 6.21. Found: C, 55.7; H, 4.48; N, 6.05. ³¹P{¹H} NMR (161.8 MHz, CD₂-Cl₂): δ 59.9 (ps t), 12.3 (AB pattern). ¹H NMR (399.8 MHz, CD₂-Cl₂): δ 7.58–7.55 (m, 4H), 7.44–7.41 (m, 2H), 7.33–7.30 (m, 4H), 6.79 (br s, 4H, H_α), 6.11 (br s, 4H, H_β), 4.69 (ps t, 2H, CH₂).

Synthesis of [Pd₂Cl₂(μ-L)₂] **5**. [Pd₂(dba)₃]·CHCl₃ (0.162 g, 0.16 mmol) was added to a dichloromethane solution of **4** (0.286 g, 0.32 mmol) with stirring, giving a slow lightening of color to red. Addition of hexane precipitated a red powder, which was washed with small amounts of dichloromethane and dried under reduced pressure. Crystallization from dichloromethane–hexane gave deep red crystals. Yield: 0.298 g (93%). Anal. Calcd for C₄₂H₄₀Cl₂N₄P₄-Pd₂: C, 50.0; H, 4.00; N, 5.56. Found: C, 50.1; H, 4.19; N, 5.20. ³¹P{¹H} NMR (161.8 MHz, CD₂Cl₂): see main text. ¹H NMR (399.8 MHz, CD₂Cl₂): δ 7.53–7.26 (m, 20H), 7.05 (m, 4H), 6.93 (m, 4H), 6.30 (m, 4H), 6.21 (m, 4H), 4.57–4.45 (m, 4H).

Synthesis of [Pd₂Cl₂(CH₃)₂(μ-L)₂] **6**. [PdCl(CH₃)(cod)] (0.340 g, 1.28 mmol) was added to a dichloromethane solution of **L** (0.463 g, 1.28 mmol). The mixture was stirred for 4 h, and then hexane was added to precipitate a colorless powder. After separation by filtration, the powder was washed with hexane and dried under reduced pressure. Crystallization from dichloromethane–hexane gave colorless crystals. Yield: 0.630 g (95%). Anal. Calcd for C₄₄H₄₆Cl₂N₄P₄Pd₂·CH₂Cl₂: C, 48.1; H, 4.31; N, 4.99. Found: C, 48.4; H, 4.56; N, 4.92. ³¹P{¹H} NMR (161.8 MHz, CDCl₃): see main text. ¹H NMR (399.8 MHz, CDCl₃): δ 7.59–7.56 (m), 7.37–7.26 (m), 6.87 (br s), 6.33 (br s), 6.15 (br s), 4.62 (br m), 4.35 (br m), 1.24 (ps t), 0.64 (ps t), 0.15 (ps t).

Synthesis of [Pd₂(CH₃)₂(μ-Cl)(μ-L)₂] **7**. TlPF₆ (0.045 g, 0.13 mmol) was added to a dichloromethane solution of **6** (0.120 g, 0.12 mmol). The mixture was stirred for 2 h with the formation of a colorless precipitate of TlCl. This was removed by filtration, and the solvent was removed from the filtrate under reduced pressure to give a yellow powder. The product was recrystallized from dichloromethane–hexane. Yield: 0.123 g (93%). Anal. Calcd for C₄₄H₄₆ClF₆N₄P₅Pd₂·³/₄CH₂Cl₂: C, 44.4; H, 3.95; N, 4.62. Found: C, 44.4; H, 3.92; N, 4.60. ³¹P{¹H} NMR (161.8 MHz, CD₂Cl₂): δ 83.8 (m, HH), 82.1 (dd, *J* 476 Hz, *J* 69 Hz, HT), 15.9 (dd, *J* 476 Hz, *J* 69 Hz, HT), 15.2 (m, HH), –143.0 (sept, PF₆, ¹J_{PF} 711 Hz). ¹H NMR (399.8 MHz, CD₂Cl₂): δ 7.87–7.76 (m), 7.64–7.51 (m), 7.50–7.42 (m), 7.36 (ps quin, C_α), 7.31–7.25 (m), 7.19–7.14 (m), 7.11 (ps quin, C_α), 6.62–6.61 (m, C_β), 6.58–6.57 (m, C_β), 6.55–6.51 (m), 6.44–6.35 (m), 4.38–4.28 (br m, CH₂), 4.24 (ps quin, CH₂), 4.13–4.03 (br m, CH₂), 1.01 (ps t, CH₃, HH), 0.86 (ps t, CH₃, HT), 0.71 (ps t, CH₃, HH).

Formation of [Ru₂Cp*₂(μ-Cl)₂(μ-L)] **8**. [RuCp*(μ₃-Cl)]₄ (0.220 g, 0.20 mmol) was added with stirring to a THF solution of **L** (0.147 g, 0.41 mmol). The resulting dark orange solution was stirred for

24 h and hexane added to precipitate an orange powder. Crystallization by slow evaporation of a dichloromethane–hexane solution produced dark orange crystals. Yield: 0.331 g (90%). Anal. Calcd for C₄₁H₅₀Cl₂N₂P₂Ru₂: C, 54.4; H, 5.56; N, 3.09. Found: C, 54.7; H, 5.59; N, 3.23. ³¹P{¹H} NMR (161.8 MHz, C₆D₆): δ 119.1 (d, ²J_{PP} 24 Hz), 34.6 (d, ²J_{PP} 24 Hz). ¹H NMR (399.8 MHz C₆D₆): δ 7.60–7.55 (m, 4H, Ph), 7.06–7.01 (m, 6H, Ph), 6.77 (ps quin, 4H, C_α), 6.09–6.08 (m, 4H, C_β), 3.92 (ps t, 2H, CH₂), 1.41 (d, 15H, ³J_{HP} 2.0 Hz, CH₃), 1.32 (d, 15H, ³J_{HP} 2.0 Hz, CH₃).

Isolation of [Rh₂(cod)₂(μ-Cl)(μ-L)]PF₆ **9**. NH₄PF₆ (0.110 g, 0.67 mmol) was added to a dichloromethane solution of [Rh(cod)-(μ-Cl)]₂ (0.166 g, 0.34 mmol) and **L** (0.244 g, 0.67 mmol). The mixture was stirred for 2 h and filtered to removed the white precipitate of NH₄Cl. The solvent was removed under reduced pressure to give an orange powder, which was washed with diethyl ether and dried under reduced pressure. Crystallization by slow diffusion of hexane in a dichloromethane solution gave an orange powder and small yellow crystals of **9**, which were separated manually. ³¹P{¹H} NMR (109.4 MHz, CD₂Cl₂): δ 109.2 (dd, ¹J_{PRh} 218 Hz, ²J_{PP} 72 Hz), 25.8 (dd, ¹J_{PRh} 145 Hz, ²J_{PP} 72 Hz), –143.0 (sept, PF₆, ¹J_{PF} 711 Hz). ¹H NMR (270.2 MHz CD₂Cl₂): δ 7.80–7.45 (m, 10H, H_o, H_p, H_m), 6.95 (ps quin, 4H, C_α), 6.52–6.46 (m, 4H, C_β), 5.20–5.05 (m, 4H, cod), 3.72–3.64 (m, 2H, CH₂), 3.28–3.05 (m, 4H, cod), 2.36–1.75 (m, 4H, cod).

Crystallography. Crystallographic data for compounds **2**·CHCl₃, **3**·CH₂Cl₂, **4**, **5**·¹/₄CH₂Cl₂, **6**, **7**·2CH₂Cl₂, **8** and **9**·CH₂Cl₂ are summarized in Table 8. Data were collected on a Nonius KappaCCD diffractometer throughout. Full matrix anisotropic refinement was implemented in the final least-squares cycles for all structures with the specific exceptions described below. All data were corrected for Lorentz and polarization. Absorption corrections (multiscan) were applied on merit to data for **2**·CHCl₃, **4**, **5**·¹/₄CH₂Cl₂, **6**, **7**·2CH₂Cl₂, and **9**·CH₂Cl₂ (maximum, minimum transmission factors were 1.00, 0.87; 1.00, 0.94; 0.80, 0.74; 0.89, 0.80; 0.84, 0.75; and 0.94, 0.88, respectively). Hydrogen atoms were included at calculated positions throughout with the exceptions of those specifically mentioned below.

In **2**·CHCl₃, the chloroform molecule was found to be disordered over two sites in the occupancy ratio 3:2, with one common chlorine atom [Cl(3)]. Efforts to model three-way disorder in this solvent because of the proximity of the largest positive peak in the difference Fourier electron density map to Cl(5) were abandoned as they had a detrimental effect on convergence of the model. The structure of **4**, where the asymmetric unit contains two crystallographically independent molecule halves, refined routinely. In **5**·¹/₄CH₂Cl₂, the pyrrolyl rings on P(3) exhibited disorder in a 1:1 ratio with the phenyl rings attached to P(4). Disordered rings were treated as rigid groups in the latter stages of refinement. The included solvent fragment, proximate to the inversion center, is disordered, and consequently the hydrogens on this fragment were not included in the model. The structure of **7**·2CH₂Cl₂ was successfully refined using a twin law which involves a 180° rotation about the 1 0 0 reciprocal lattice vector. This twin law was determined using ROTAX,²³ followed by use of WinGX²⁴ to output the data in SHELXL-97, HKLF 5 format.

Analysis of the data for structure **8** led to initial solution in space group *P2*₁/*n* with severe disorder of the Cp* rings which could not be successfully modeled in any sensible manner. However, while reflection intensities in the data set suggesting the presence of an

(23) Cooper, R. I.; Gould, R. O.; Parsons, S.; Watkin, D. J. *J. Appl. Crystallogr.* **2002**, *35*, 168–174.

(24) Farrugia, L. J. *J. Appl. Crystallogr.* **1999**, *32*, 837–838.

n glide perpendicular to b were weak, they were undeniably observed. Thus, the structure as presented here converged optimally as a racemic twin, in space group $P2_1$ with two molecules in the asymmetric unit. The asymmetric unit in $\mathbf{9} \cdot \text{CH}_2\text{Cl}_2$ consists of half a dimeric cation with C(19) and Cl(1) located on a 2-fold crystallographic rotation axis, half of a PF_6^- anion with the phosphorus located on an inversion center, and half of a molecule of dichloromethane. The solvent chlorine was disordered over two positions in a 1:1 ratio, with the carbon atom therein also located on a 2-fold axis. Hence, the methylene hydrogens were not included in the refinement. As in $\mathbf{5} \cdot \frac{1}{4}\text{CH}_2\text{Cl}_2$, the pyrrolyl and phenyl groups in the cation were disordered in a 1:1 ratio between the phosphines. These rings were treated as rigid groups in the latter stages of refinement where atomic displacement parameters therein were also restrained. Hydrogen atoms were included at calculated positions except for H(19) and the cyclooctadiene alkenic hydrogens. These exceptions were readily located in the penultimate difference Fourier electron density map, and refined at a distance of 0.90 Å from the relevant parent atoms.

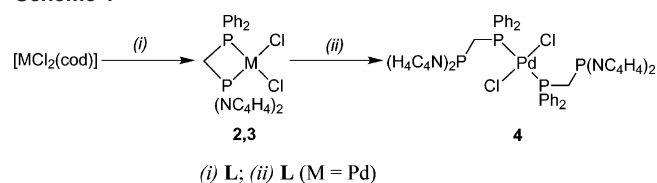
Results and Discussion

Synthesis and Reactivity of $\text{Ph}_2\text{PCH}_2\text{P}(\text{NC}_4\text{H}_4)_2$ **L.** $\text{Ph}_2\text{PCH}_2\text{P}(\text{NC}_4\text{H}_4)_2$ **L** was prepared in a two-step procedure starting from PMePh_2 . The first step involved conversion of PMePh_2 into $\text{Ph}_2\text{PCH}_2\text{Li}$ by reaction with BuLi in the presence of TMEDA.²¹ $\text{Ph}_2\text{PCH}_2\text{Li}$ was isolated as a colorless powder, and a THF solution of this was added dropwise to a THF–hexane solution containing 1 equiv of $\text{PCl}(\text{NC}_4\text{H}_4)_2$,¹¹ to give **L** as a colorless powder following recrystallization from THF–hexane. The $^{31}\text{P}\{^1\text{H}\}$ NMR spectrum of **L** consists of two doublets at δ 66.1 and δ –25.5, with $^2J_{\text{PP}}$ 147 Hz. The lower field signal can be assigned to the di(*N*-pyrrolyl)phosphino group on the basis of its chemical shift, by comparison with $\text{PPh}(\text{NC}_4\text{H}_4)_2$ (δ 70.6).⁹ The ^1H NMR spectrum of **L** showed a characteristic pseudo-quintet and pseudo-triplet for the protons of the pyrrolyl rings and two multiplets for the protons of the phenyl rings. The signal for the protons of the methylene bridge appeared as a doublet of doublets at δ 3.18 with $^2J_{\text{HP}}$ 6.0 and 1.6 Hz. In the $^{13}\text{C}\{^1\text{H}\}$ NMR spectrum the signal assigned to the methylene carbon was observed as a doublet of doublets at δ 31.0 with $^1J_{\text{CP}}$ 26 and 20 Hz.

The order of addition in the second step proved to be important in optimizing the yield of **L**. Addition of $\text{PCl}(\text{NC}_4\text{H}_4)_2$ to $\text{Ph}_2\text{PCH}_2\text{Li}$ led to significant amounts of a byproduct, whose $^{31}\text{P}\{^1\text{H}\}$ NMR spectrum consists of a triplet (δ 39.6) and a doublet (δ –23.4) with $^2J_{\text{PP}}$ 126 Hz and in the intensity ratio 1:2. The spectrum is consistent with this compound being $(\text{Ph}_2\text{PCH}_2)_2\text{P}(\text{NC}_4\text{H}_4)$, formed by reaction of **L** with a second equivalent of $\text{Ph}_2\text{PCH}_2\text{Li}$.

L was found to be moderately air-stable, and the P–N bonds are stable to methanolysis at ambient temperature in contrast to those in $(\text{H}_4\text{C}_4\text{N})_2\text{P}\{\text{NC}_4\text{H}_3\text{C}(\text{O})\text{Me}-2\}$.¹¹ Although **L** is not prone to aerial oxidation, the differential reactivity of the two phosphino groups can be witnessed by its reaction with sulfur. On stirring a dichloromethane solution of **L** with excess sulfur for 4 h, full conversion to $\text{Ph}_2\text{P}(\text{S})\text{CH}_2\text{P}(\text{NC}_4\text{H}_4)_2$ **1** was achieved. The $^{31}\text{P}\{^1\text{H}\}$ NMR spectrum for **1** contained two doublets at δ 56.8 and δ 36.6,

Scheme 1



with $^2J_{\text{PP}}$ 85 Hz. The doublet at δ 56.8 can be assigned to the di(*N*-pyrrolyl)phosphino group and is shifted only slightly with respect to **L**. In contrast, the signal at δ 36.6 is shifted considerably downfield with respect to the PPh_2 signal in **L**, and is consistent with the selective oxidation of this phosphorus atom. The NMR parameters observed for **1** are comparable with those previously reported for $\text{Ph}_2\text{P}(\text{S})\text{CH}_2\text{PPh}_2$ for which doublets at δ 39.2 and δ –29.1 with $^2J_{\text{PP}}$ 74 Hz were observed.²⁵ In the IR spectrum of **1** $\nu(\text{PS})$ was observed at 625 cm^{-1} , in the anticipated region.²⁶

Synthesis and Characterization of the Chelate Complexes $[\text{MCl}_2(\text{L}-\kappa^2\text{P},\text{P}')] (M = \text{Pd}, \text{Pt})$. The reaction of 1 equiv of **L** with $[\text{MCl}_2(\text{cod})]$ (M = Pd, Pt) in dichloromethane gave the complexes $[\text{PdCl}_2(\text{L}-\kappa^2\text{P},\text{P}')] \mathbf{2}$ and $[\text{PtCl}_2(\text{L}-\kappa^2\text{P},\text{P}')] \mathbf{3}$, respectively, in good yields (Scheme 1). Both complexes were isolated as air-stable crystalline materials and fully characterized by multinuclear NMR spectroscopy, microanalysis, and single-crystal X-ray analyses.

The $^{31}\text{P}\{^1\text{H}\}$ NMR spectrum of **2** consisted of two doublets, at δ 0.0 and δ –46.7, with $^2J_{\text{PP}}$ 84 Hz. The higher field signal can be assigned to the diphenylphosphino group on the basis of the chemical shift, which is similar to that observed for $[\text{PdCl}_2(\text{dppm}-\kappa^2\text{P},\text{P})]$ (δ –53.7²⁷). In addition, the lower field signal is broader, which is consistent with bonding to the quadrupolar nitrogen atoms.⁹ The upfield shift of the signals with respect to the free ligand is typical of a four-membered chelate ring.²⁸ In the ^1H NMR spectrum, the methylene hydrogen atoms were observed as a doublet of doublets at δ 4.54.

The $^{31}\text{P}\{^1\text{H}\}$ NMR spectrum of **3** consisted of two doublets with ^{195}Pt satellites, at δ –16.5 ($^1J_{\text{PPt}}$ 3932 Hz, $^2J_{\text{PP}}$ 75 Hz) and δ –57.0 ($^1J_{\text{PPt}}$ 2951 Hz), respectively. As with **2** the higher field signal can be assigned to the diphenylphosphino group, and is close to the resonance observed for the dppm analogue $[\text{PtCl}_2(\text{dppm}-\kappa^2\text{P},\text{P})]$ (δ –64.3, $^1J_{\text{PPt}}$ 3078 Hz).²⁹ The larger $^1J_{\text{PPt}}$ coupling constant observed for the di(*N*-pyrrolyl)phosphino group is consistent with this being a better π -acceptor than the diphenylphosphino group. The methylene hydrogen atoms were observed in the ^1H NMR spectrum as a doublet of doublets at δ 4.60 with ^{195}Pt satellites.

Single crystals of **2** and **3** were grown by slow diffusion of hexane into chloroform and dichloromethane solutions, respectively. The X-ray crystal structures of **2**· CHCl_3 and **3**· CH_2Cl_2 confirmed the chelating coordination mode of **L**.

(25) Blagborough, T. C.; Davis, R.; Ivison, P. *J. Organomet. Chem.* **1994**, *467*, 85–94.

(26) Birdsall, D. J.; Slawin, A. M. Z.; Woollins, J. D. *Polyhedron* **2001**, *20*, 125–134.

(27) Oliver, D. L.; Anderson, G. K. *Polyhedron* **1992**, *11*, 2415–2420.

(28) Garrou, P. E. *Chem. Rev.* **1981**, *81*, 229–266.

(29) Appleton, T. G.; Bennett, M. A.; Tomkins, I. B. *J. Chem. Soc., Dalton Trans.* **1976**, 439.

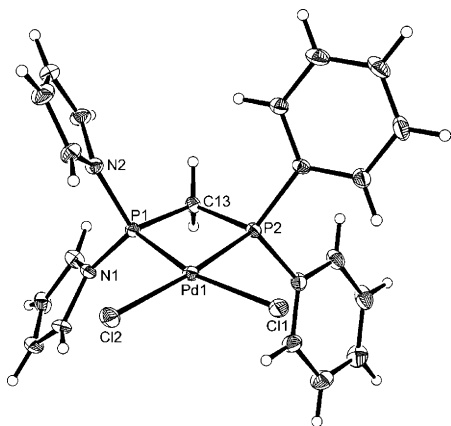


Figure 1. Molecular structure of $[\text{PdCl}_2(\text{L-}\kappa^2\text{P,P}')\cdot\text{CHCl}_3]$ ($2\cdot\text{CHCl}_3$) with the included solvent omitted for clarity and thermal ellipsoids shown at the 30% probability level.

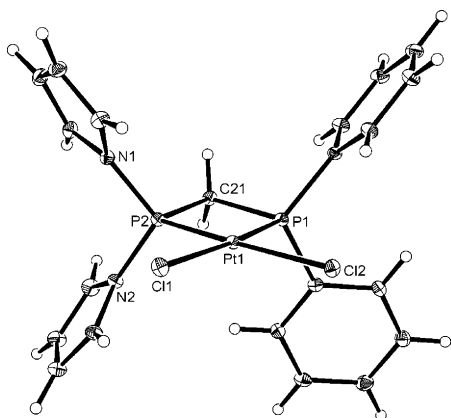


Figure 2. Molecular structure of $[\text{PtCl}_2(\text{L-}\kappa^2\text{P,P}')\cdot\text{CH}_2\text{Cl}_2]$ ($3\cdot\text{CH}_2\text{Cl}_2$) with the included solvent omitted for clarity and thermal ellipsoids shown at the 30% probability level.

Table 1. Selected Bond Lengths (Å) and Angles (deg) for Complexes $2\cdot\text{CHCl}_3$ and $3\cdot\text{CH}_2\text{Cl}_2$

	$2\cdot\text{CHCl}_3$		$3\cdot\text{CH}_2\text{Cl}_2$
Pd(1)–P(1)	2.2109(13)	Pt(1)–P(2)	2.1877(7)
Pd(1)–P(2)	2.2347(13)	Pt(1)–P(1)	2.2372(7)
Pd(1)–Cl(1)	2.3273(13)	Pt(1)–Cl(2)	2.3445(7)
Pd(1)–Cl(2)	2.3540(13)	Pt(1)–Cl(1)	2.3667(7)
P(1)–N(1)	1.673(4)	P(2)–N(1)	1.681(2)
P(1)–N(2)	1.689(5)	P(2)–N(2)	1.682(3)
P(1)–C(13)	1.814(5)	P(2)–C(21)	1.822(3)
P(2)–C(13)	1.850(5)	P(1)–C(21)	1.856(3)
P(1)–Pd(1)–P(2)	73.36(5)	P(1)–Pt(1)–P(2)	73.32(3)
P(1)–Pd(1)–Cl(2)	100.55(5)	P(1)–Pt(1)–Cl(2)	97.47(3)
P(2)–Pd(1)–Cl(1)	91.77(5)	P(2)–Pt(1)–Cl(1)	98.51(3)
Cl(1)–Pd(1)–Cl(2)	94.29(5)	Cl(1)–Pt(1)–Cl(2)	90.69(2)
P(1)–Pd(1)–Cl(1)	164.97(5)	P(1)–Pt(1)–Cl(1)	171.80(3)
P(2)–Pd(1)–Cl(2)	173.88(5)	P(2)–Pt(1)–Cl(2)	170.65(3)
P(1)–C(13)–P(2)	92.9(2)	P(1)–C(21)–P(2)	91.85(13)

Selected bond lengths and angles are reported in Table 1, and the structures are shown in Figures 1 and 2. In both **2** and **3** the metal adopts a distorted square planar coordination geometry, with **L** assuming bite angles of $73.36(5)^\circ$ and $73.32(3)^\circ$, respectively. In both cases the M–P bond to the di(*N*-pyrrolyl)phosphino group is significantly shorter than that to the diphenylphosphino group [Pd–P 2.2109(13), 2.2347(13) Å in **2**; Pt–P 2.1877(7), 2.2372(7) Å in **3**], which is consistent with the stronger π -acceptor ability of the

$\text{P}(\text{NC}_4\text{H}_4)_2$ group. However, significant differences in the two Pd–P bond lengths in $[\text{PdCl}_2(\text{dppm-}\kappa^2\text{P,P}')]$ [2.234(1) and 2.250(1) Å]³⁰ suggest that the electronic difference between the phosphino groups in the structures of **2** and **3** may not be the only factor involved in the M–P bond length difference. Notably, though, the bond distances between the methylene carbon and the two phosphorus atoms in **2** and **3** are also different. In both cases the bond to the phosphorus atom of the diphenylphosphino group [P(2)–C(13) 1.850(5) Å in **2** and P(1)–C(21) 1.856(3) Å in **3**] is longer than that to the phosphorus atom of the di(*N*-pyrrolyl)phosphino group [P(1)–C(13) 1.814(5) Å in **2**, P(2)–C(21) 1.822(3) Å in **3**].

There is a difference in the orientation of the two aromatic ring types in **2** and **3**, with the pyrrolyl rings facing each other and the phenyl rings twisted. In the supramolecular structures, one of the phenyl rings from each molecule is directed into the cleft between the pyrrolyl rings in a neighboring molecule. Moreover, the disordered chloroform solvate molecule in **2** forms C–H \cdots Cl hydrogen bonds with the coordinated chlorides [C(24) \cdots Cl(2) 3.460 Å, H(24)–Cl(2) 2.55 Å, C(24)–H(24) \cdots Cl(2) 151° ; C(24) \cdots Cl(1) 3.446 Å, H(24) \cdots Cl(1) 2.57 Å, C(24)–H(24) \cdots Cl(1) 146°].

Reaction of L with $[\text{MCl}_2(\text{L-}\kappa^2\text{P,P}')]$ (M = Pd, Pt). The addition of an additional 1 equiv of **L** to a dichloromethane solution of **2** led to the disappearance of the pair of doublets in the $^{31}\text{P}\{^1\text{H}\}$ NMR spectrum and the appearance of a more complex pattern. This spectrum consisted of a broad pseudo-triplet at δ 59.9 and an AB pattern at δ 12.3, and was identified as arising from an $[\text{AX}]_2$ spin system^{31,32} with the broadness in the pseudo-triplet a consequence of the nitrogen quadrupoles. The increase in chemical shift of both signals from those observed for **2** suggested that the four-membered ring was no longer present, whereas the proximity of the lower field resonance to that for **L** suggested that the di(*N*-pyrrolyl)phosphino groups were uncoordinated. Hence the product from the reaction of **2** with **L** was identified as *trans*- $[\text{PdCl}_2(\text{L-P})_2]$ **4** (Scheme 1), which could be isolated following recrystallization from dichloromethane–hexane. The large value of the *trans* $^2J_{\text{PP}}$ coupling constant between the diphenylphosphino groups together with a small but nonzero $^4J_{\text{PP}}$ coupling between the diphenylphosphino and di(*N*-pyrrolyl)phosphino phosphorus nuclei is the origin of the appearance of the spectrum. The ^1H NMR spectrum of **4** shows the signal for the methylene protons of **L** at δ 4.69 as a *pseudo* triplet due to the two $^2J_{\text{HP}}$ coupling constants having very similar values. Variable temperature $^{31}\text{P}\{^1\text{H}\}$ and ^1H NMR spectra (room temperature to -70°C) showed no variation, suggesting that **4** is static on the NMR time scale.

Complex **4** can also be prepared directly from the reaction of $[\text{PdCl}_2(\text{cod})]$ and 2 equiv of **L**. In addition to the signals above, crude reaction mixtures showed the presence of two

(30) Steffen, W. L.; Palenik, G. J. *Inorg. Chem.* **1976**, *15*, 2432–2439.

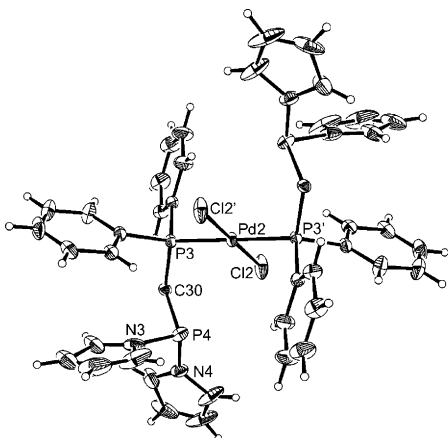
(31) Becker, E. D. *High-resolution NMR spectroscopy*; Academic Press: New York, 1969.

(32) Akitt, J. W.; Mann, B. E. *NMR and chemistry: an introduction to modern NMR spectroscopy*, 4th ed.; Stanley Thorne: Cheltenham, U.K., 2000.

Table 2. Selected Bond Lengths (Å) and Angles (deg) for Complex **4**^a

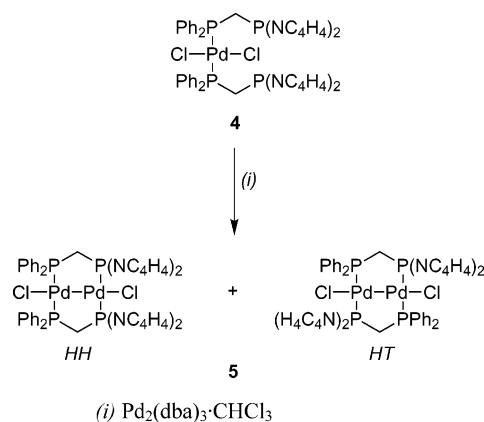
Pd(1)–P(1)	2.3361(10)	Pd(2)–P(3)′	2.3196(10)
Pd(1)–Cl(1)	2.3077(10)	Pd(2)–Cl(2)	2.3000(12)
P(1)–C(9)	1.842(4)	P(3)–C(30)	1.833(4)
P(2)–C(9)	1.850(4)	P(4)–C(30)	1.839(4)
P(2)–N(1)	1.731(4)	P(4)–N(3)	1.702(5)
P(2)–N(2)	1.712(4)	P(4)–N(4)	1.729(4)
Cl(1)–Pd(1)–P(1)′	91.94(4)	Cl(2)–Pd(2)–P(3)″	94.11(4)
Cl(1)–Pd(1)–P(1)	88.06(4)	P(1)–C(9)–P(2)	115.1(2)
Cl(2)–Pd(2)–P(3)	85.89(4)	P(3)–C(30)–P(4)	110.9(2)

^a Primed atoms generated by the symmetry operation $-x + 2, y + 2, z$. Double primed atoms generated by the symmetry operation $-x + 1, y + 2, z + 1$.

**Figure 3.** Molecular structure of one of the independent molecules of *trans*-[PdCl₂(L-P)₂] **4** with thermal ellipsoids shown at the 30% probability level.

broad signals. These resonances were found to be temperature dependent, and on cooling to -66 °C they were observed as sharp doublets at δ 56.4 and δ 28.2, with $^2J_{PP}$ 100 Hz. These values are consistent with this compound being *cis*-[PdCl₂(L-P)₂]. The spectrum of *cis*-[PdCl₂(L-P)₂] is simpler than that of the *trans* isomer **4** due to the negligible value of $^4J_{PP}$. As a consequence of this the two diphenylphosphino groups are magnetically equivalent and the spin system is A₂X₂.

The identity of **4** as *trans*-[PdCl₂(L-P)₂] was confirmed by a single-crystal X-ray analysis. Suitable crystals were obtained following recrystallization from dichloromethane–hexane, and two crystallographically independent half-molecules were observed in the asymmetric unit. Each molecule contains a crystallographically imposed center of symmetry at the palladium atom, and, consistent with the NMR data, the diphenylphosphino group is coordinated while the di(*N*-pyrrolyl)phosphino group is pendant. The metal geometry is distorted square planar, with bond lengths and angles very similar for the two independent units, and *cis* angles in the range 85.89(4)–94.11(4)°. Selected bond lengths and angles for both independent molecules are given in Table 2, and one of the molecules is depicted in Figure 3. The major difference between the independent molecules lies in the position of the uncoordinated di(*N*-pyrrolyl)phosphino groups. The Pd⋯P distances to the uncoordinated phosphorus atoms are 4.739 and 3.638 Å, and in the latter case the phosphorus lone pair appears to be directed toward the metal center.

Scheme 2

The generation of *trans*-[PdCl₂(L-P)₂] **4** from **2** involves cleavage of the Pd–P(NC₄H₄)₂ bond, so the reaction shows selective cleavage of the shorter Pd–P bond. In contrast to this reaction, the platinum analogue **3** does not react with **L**. The reaction of 2 equiv of **L** with [PtCl₂(cod)] produced a number of products as evidenced by the ³¹P{¹H} spectrum, and it did not prove possible to isolate *trans*-[PtCl₂(L-P)₂] or any other compound from this reaction mixture.

Reactions of [PdCl₂(L-κ¹P)₂]. The complex [PdCl₂(L-κ¹P)₂] **4** possesses two pendant di(*N*-pyrrolyl)phosphino groups and, thus, has the potential to form homo- or heterometallic dimers. The reaction of **4** with [PdCl₂(cod)] gave only complex **2**, suggesting that dimeric palladium complexes with bridging **L** and terminal chloride are less stable than those with chelating **L**. This behavior resembles that of dppm for which the face-to-face dimer [Pd₂Cl₄(μ-dppm)₂] isomerizes to the chelate complex [PdCl₂(dppm-κ²P,P)].³³ Similarly, the reaction of **4** with [PtCl₂(cod)] gave a 1:1 mixture of complexes **2** and **3** rather than a mixed metal dimer.

In contrast to these observations, the reaction of **4** with [Pd₂(dba)₃]·CHCl₃ gave a red complex **5**, the ³¹P{¹H} NMR spectrum of which consisted of two complex groups of signals at δ 68.6 to 63.2 and δ -5.2 to -10.5 , similar in appearance, with each group containing 13 lines: too many for the spectrum to be derived from a simple [AX]₂ spin system. In addition, the relative movement of some of the lines within each group upon changes in concentration or temperature suggested that they did not comprise one single multiplet. The spectrum was interpreted as being composed of two overlapping [AX]₂ spin systems, from the product [Pd₂Cl₂(μ-L)₂] existing as both head-to-head (HH) and head-to-tail (HT) isomers (Scheme 2). In the HH isomer the two palladium centers are different, one being coordinated to two PPh₂ groups and the other to two P(NC₄H₄)₂ groups, whereas in the HT isomer both are identical, being coordinated to one PPh₂ group and one P(NC₄H₄)₂ group.

Of the two 13-line patterns, that at lower field can be assigned to the P(NC₄H₄)₂ groups and that at higher field to the PPh₂ groups. The lower field pattern is shown in Figure 4 together with simulations for the HH and HT isomers.

(33) Hunt, C. T.; Balch, A. L. *Inorg. Chem.* **1981**, *20*, 2267–2270.

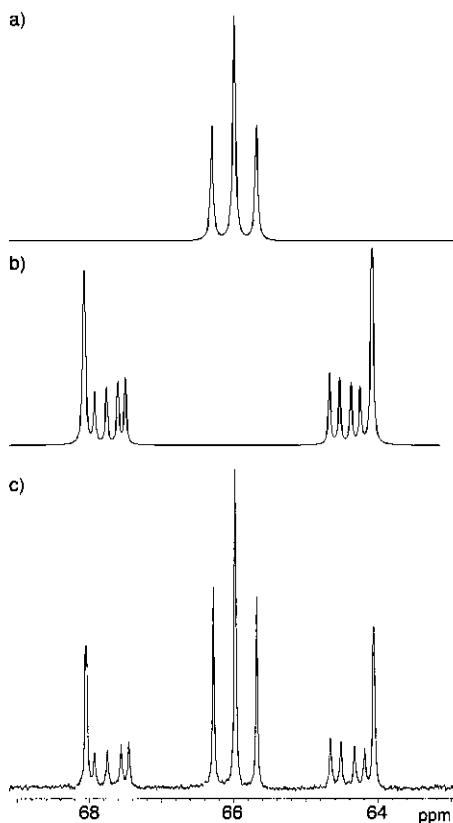


Figure 4. Low-field part of the $^{31}\text{P}\{^1\text{H}\}$ NMR spectrum of $[\text{Pd}_2\text{Cl}_2(\mu\text{-L})_2]$ **5** (c) together with simulations for the HH (a) and HT (b) isomers.

Although both isomers give rise to $[\text{AX}]_2$ multiplets, their appearances are very different due to the relative magnitudes of the coupling constants. The central pseudo-triplet can be assigned to the HH isomer in which $^2J(\text{AA}')$ and $^2J(\text{XX}')$ [$\text{A} = \text{P}(\text{NC}_4\text{H}_4)_2$, $\text{X} = \text{PPh}_2$] are considerably larger than all the other coupling constants. The observation of only these three lines precludes a full spectral analysis. The remaining 10 lines result from the HT isomer, and in this case a full analysis is possible, giving $^2J(\text{AX})$ 60 Hz, $^2J(\text{AX}')$ 582 Hz, $^3J(\text{XX}')$ 23 Hz, and $^3J(\text{AA}')$ 53 Hz. The spectral parameters obtained for the HT isomer are similar to those reported for the complex $[\text{PdCl}_2(\mu\text{-dppm})\{\mu\text{-Ph}_2\text{PCH}(\text{CH}_3)\text{PPh}_2\}]$, for which $^2J_{\text{PP}}$ through the metal is 440 Hz.³⁴ The $^{31}\text{P}\{^1\text{H}\}$ NMR spectrum of **5** recorded at both high and low temperature in $\text{C}_2\text{D}_2\text{Cl}_4$ shows no significant changes, suggesting no inter-conversion of the isomers in solution.

Orange single crystals of $5 \cdot 1/4\text{CH}_2\text{Cl}_2$ were grown from the slow diffusion of hexane into a dichloromethane solution of **5**. The compound crystallized as a 1:1 mixture of the HH and HT isomers, together with a small amount of disordered solvent. The co-crystallization of the isomers results in one of the **L** ligands being disordered, with the phenyl and *N*-pyrrolyl rings present on both ends with 50% occupancy. Selected bond distances and angles are reported in Table 3, and the structure of one of the isomers is shown in Figure 5. The Pd(1)–Pd(2) distance of 2.6344(5) Å indicates the presence of a Pd–Pd bond, which is in agreement with the

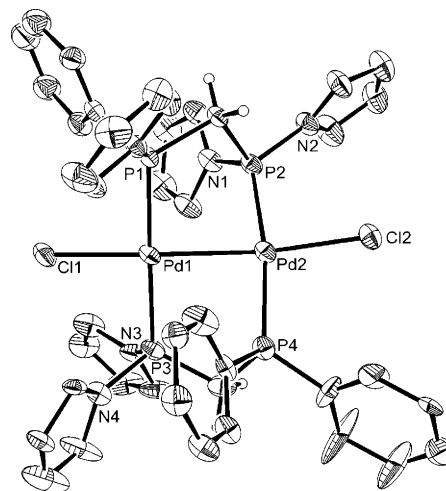


Figure 5. Molecular structure of the HT isomer of $[\text{Pd}_2\text{Cl}_2(\mu\text{-L})_2] \cdot 1/4\text{CH}_2\text{Cl}_2$ ($5 \cdot 1/4\text{CH}_2\text{Cl}_2$) with the phenyl and pyrrolyl protons and included solvent omitted for clarity and thermal ellipsoids shown at the 30% probability level.

Table 3. Selected Bond Lengths (Å) and Angles (deg) for Complex $5 \cdot 1/4\text{CH}_2\text{Cl}_2$

Pd(1)–Pd(2)	2.6344(5)	Pd(2)–Cl(2)	2.4041(13)
Pd(1)–P(1)	2.3179(11)	P(1)–C(41)	1.844(4)
Pd(1)–P(3)	2.2842(12)	P(2)–C(41)	1.811(4)
Pd(2)–P(2)	2.2579(13)	P(2)–N(1)	1.707(4)
Pd(2)–P(4)	2.2841(13)	P(2)–N(2)	1.718(4)
Pd(1)–Cl(1)	2.3894(13)		
P(1)–Pd(1)–Cl(1)	90.06(4)	Cl(2)–Pd(2)–P(4)	96.58(5)
Cl(1)–Pd(1)–P(3)	91.34(5)	P(4)–Pd(2)–Pd(1)	87.37(3)
P(3)–Pd(1)–Pd(2)	90.10(4)	Pd(1)–Pd(2)–P(2)	83.63(3)
Pd(2)–Pd(1)–P(1)	88.49(3)	P(4)–Pd(2)–P(2)	169.79(5)
P(1)–Pd(1)–P(3)	176.77(4)	Pd(1)–Pd(2)–Cl(2)	169.85(3)
Pd(2)–Pd(1)–Cl(1)	178.56(4)	P(1)–C(41)–P(2)	103.2(2)
P(2)–Pd(2)–Cl(2)	93.09(4)	P(4)–C(42)–P(3)	106.0(3)

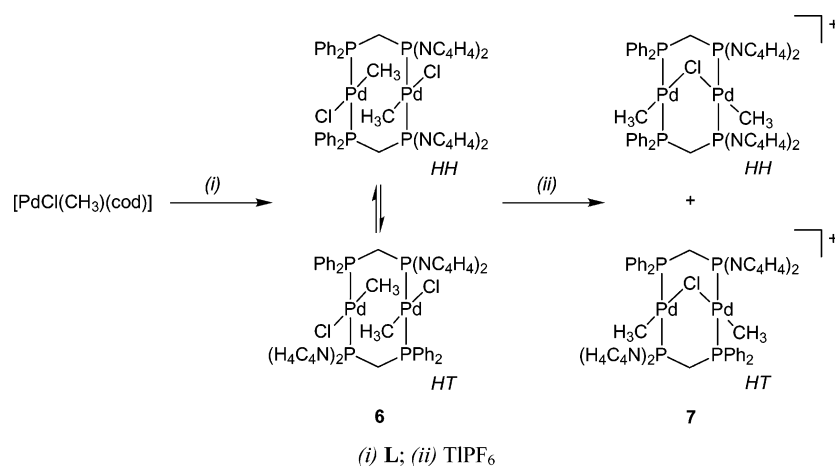
formal electron count. Both palladium centers possess distorted square planar coordination geometries with trans-coordinated phosphorus atoms. The Cl1–Pd1–Pd2–Cl2 unit is approximately linear with a torsion angle Cl(1)–Pd(1)–Pd(2)–Cl(2) of 30.0° and angles Cl(2)–Pd(2)–Pd(1) of 169.85(3)° and Pd(2)–Pd(1)–Cl(1) of 178.56(4)°. The mean coordination planes of the two palladium centers form an angle of approximately 32°. The structural parameters are similar to those reported for $[\text{Pd}_2\text{Br}_2(\mu\text{-dppm})_2]$, which also contains a distorted geometry with a twist about the Pd–Pd bond.³⁵ The Pd–Pd bond distance in this complex is 2.699(5) Å, and the distortion from planarity has been rationalized as resulting from the conflicting requirements of interaxial d orbital repulsion and accommodation of the bridging dppm ligands with minimum strain. This explanation is likely to be equally valid in the case of **5**.

Due to the disorder in **5**, the bond distances Pd(1)–P(3) [2.2842(12) Å] and Pd(2)–P(4) [2.2841(13) Å] are indistinguishable. However, for the non-disordered ligand the Pd(1)–P(1) distance [2.3179(11) Å] to the diphenylphosphino group is longer than the Pd(2)–P(2) distance [2.2579(13) Å] to the di(*N*-pyrrolyl)phosphino group.

(34) Lee, C.-L.; Yang, Y.-P.; Rettig, S. J.; James, B. R.; Nelson, D. A.; Lilga, M. A. *Organometallics* **1986**, *5*, 2220–2228.

(35) Holloway, R. G.; Penfold, B. R.; Colton, R.; McCormick, M. J. *J. Chem. Soc., Chem. Commun.* **1976**, 485–486.

Scheme 3



Synthesis of [Pd₂Cl₂(CH₃)₂(μ-L)₂]. The reaction of 1 equiv of **L** with [PdCl(CH₃)(cod)] produced [Pd₂Cl₂(CH₃)₂(μ-L)₂] **6**, which was characterized by multinuclear NMR spectroscopy, microanalysis and X-ray crystallography. As with **5**, complex **6** exists in solution as a mixture of HH and HT isomers (Scheme 3). However, the HT isomer prevails at low temperature and crystallizes preferentially.

The ³¹P{¹H} NMR spectrum of **6** recorded at ambient temperature showed a number of broad resonances, consistent with the presence of both HH and HT isomers; however, at -80 °C the spectrum consisted solely of two doublets of doublets at δ 80.3 and δ 17.4, both with coupling constants of 468 and 72 Hz. The low-temperature spectrum can be interpreted by considering it a special case of the [AX]₂ spin system in which *J*(AA') and *J*(XX') are very small or equal to zero. This suggests that the compound exists solely as the HT isomer at this temperature, and that in this dimer there is no bond between the two palladium atoms, which was subsequently confirmed by the crystallographic analysis.

The NMR data indicates that the HT and HH isomers are in equilibrium with the proportion of the HH isomer increasing with the temperature. This was verified by recording ³¹P{¹H} NMR spectra at higher temperatures, and at 80 °C the HH isomer was observed to be the major species, though the spectrum also showed a significant amount of complex **5**. This is consistent with **6** being thermally unstable and decomposing with the reductive elimination of ethane to give the palladium(I) dimer **5** as a mixture of HH and HT isomers. Related reactions involving the formation of compounds such as [Pd₂(μ-Cy₂PCH₂PCy₂)₂] from [Pd(CH₃)₂(Cy₂PCH₂PCy₂-κ²P,P)] have recently been reported.³⁶

Single crystals of **6** were prepared by recrystallization from dichloromethane-hexane, and the X-ray analysis of these confirmed their identity as the HT isomer of [Pd₂Cl₂(CH₃)₂(μ-L)₂]. Selected bond angles and distances for **6** are reported in Table 4, and the complex is shown in Figure 6. The asymmetric unit consists of one half-molecule of **6**, with the remainder generated through a crystallographically imposed center of symmetry.

Table 4. Selected Bond Lengths (Å) and Angles (deg) for Complex **6**^a

Pd(1)–Cl(1)	2.4266(7)	Pd(1)–P(1)	2.2865(7)
Pd(1)–C(1)	2.064(3)	Pd(1)–P(2)'	2.3150(7)
C(1)–Pd(1)–P(2)'	90.61(8)	P(1)–Pd(1)–P(2)'	172.37(2)
P(1)–Pd(1)–C(1)	86.74(8)	C(1)–Pd(1)–Cl(1)	169.92(2)
P(1)–Pd(1)–Cl(1)	98.00(2)	P(1)–C(10)–P(2)	118.74(14)
Cl(1)–Pd(1)–P(2)'	85.77(2)		

^a Primed atoms generated by the symmetry operation $-x, -y + 1, -z + 1$.

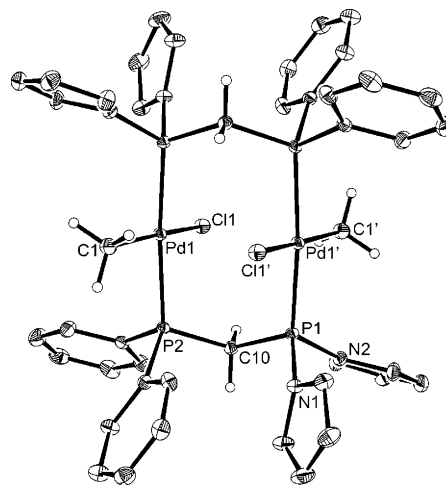


Figure 6. Molecular structure of [Pd₂Cl₂(CH₃)₂(μ-L)₂] **6** with the phenyl and pyrrolyl protons omitted for clarity and thermal ellipsoids shown at the 30% probability level.

The palladium atoms adopt distorted square-planar coordination with mutually trans phosphorus atoms, and cis angles ranging from 85.77(2)° to 98.00(2)°. The palladium mean coordination planes form an angle of approximately 70° with the plane containing the four phosphorus atoms. The Pd(1)⋯Pd(1)' distance of 3.371 Å indicates the absence of any metal–metal bonding, as expected from the NMR data and electron-counting rules. The Pd–P(NC₄H₄)₂ bond distance [Pd(1)–P(1) 2.2865(7) Å] is shorter than the Pd–PPh₂ distance [Pd(1)–P(2) 2.3150(7) Å] as observed for **2** and **3**, indicating the greater π-acceptor character of the *N*-pyrrolyl groups.

(36) Reid, S. M.; Mague, J. T.; Fink, M. J. *J. Am. Chem. Soc.* **2001**, *123*, 4081–4082.

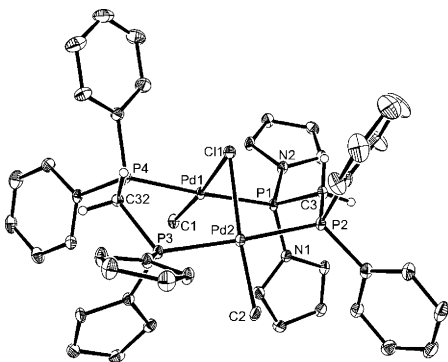


Figure 7. Molecular structure of $[\text{Pd}_2(\text{CH}_3)_2(\mu\text{-Cl})(\mu\text{-L})_2]\text{PF}_6 \cdot 2\text{CH}_2\text{Cl}_2$ ($7 \cdot 2\text{CH}_2\text{Cl}_2$) with the phenyl, pyrrolyl, and methyl protons, anion, and included solvent omitted for clarity and thermal ellipsoids shown at the 30% probability level.

Reaction of $[\text{Pd}_2\text{Cl}_2(\text{CH}_3)_2(\mu\text{-L})_2]$ with TIPF_6 . The reaction of **6** with TIPF_6 occurred with abstraction of one of the chlorides and formation of the “A-frame” complex $[\text{Pd}_2(\text{CH}_3)_2(\mu\text{-Cl})(\mu\text{-L})_2]\text{PF}_6$ **7**, with the $^{31}\text{P}\{^1\text{H}\}$ NMR spectrum showing a mixture of HH and HT isomers in the approximate ratio 1:4 (Scheme 3). The signals assigned to the HT isomer appeared as a pair of doublets of doublets centered at δ 82.1 and δ 15.9 with coupling constants of 476 and 69 Hz. As for the HT isomer of **6**, the appearance of these signals can be interpreted as being derived from a $[\text{AX}]_2$ spin system in which the 4J coupling constants $J(\text{AA}')$ and $J(\text{XX}')$ are close or equal to zero. The signals assigned to the HH isomer appeared as two complex multiplets of identical appearance centered at δ 83.8 and δ 15.2. These multiplets can be interpreted as being derived from an $[\text{AX}]_2$ spin system in which the 2J coupling constants $J(\text{AA}')$ and $J(\text{XX}')$ are much larger than all the others. Variable temperature NMR studies showed no changes in the appearance or in the relative intensities of the signals for the HH and HT isomers, indicating the absence of an equilibrium between them.

The presence of the two isomers was also apparent from the ^1H NMR spectra, in particular from the appearance of the signals from the methyl protons. These are observed as a pseudo-triplet at δ 0.86 for the HT isomer and as a pair of pseudo-triplets at δ 1.01 and δ 0.71 for the HH isomer, with coupling constants of 2 Hz.

Recrystallization of **7** by slow diffusion of hexane in a dichloromethane solution gave crystalline material that on the basis of NMR data was enriched in the HT isomer (>95:5). Further recrystallization gave crystals that, though twinned, were suitable for X-ray crystallography. The asymmetric unit contained one molecule of **7** and two molecules of dichloromethane. Analysis of the structure confirmed the presence of the HT isomer of **7**, which is shown in Figure 7. Selected bond lengths and angles are given in Table 5. The two palladium centers are distorted square planar in geometry, with cis angles in the range 84.09(3)–92.91(3) $^\circ$ and a Pd–Cl–Pd angle of 73.59(2) $^\circ$ around the bridging chloride. The Pd \cdots Pd distance of 2.9488(3) Å is somewhat shorter than those in the related dppm com-

Table 5. Selected Bond Lengths (Å) and Angles (deg) for Complex $7 \cdot 2\text{CH}_2\text{Cl}_2$

Pd(1)–P(1)	2.3127(8)	P(1)–N(1)	1.705(3)
Pd(1)–P(4)	2.3143(8)	P(1)–N(2)	1.696(3)
Pd(1)–C(1)	2.056(3)	P(3)–N(3)	1.702(3)
Pd(1)–Cl(1)	2.4589(8)	P(3)–N(4)	1.709(3)
Pd(2)–P(2)	2.3166(8)	P(1)–C(3)	1.823(3)
Pd(2)–P(3)	2.3081(8)	P(2)–C(3)	1.847(3)
Pd(2)–C(2)	2.053(3)	P(3)–C(32)	1.827(3)
Pd(2)–Cl(1)	2.4644(8)	P(4)–C(32)	1.852(3)
C(1)–Pd(1)–P(1)	92.05(9)	P(2)–Pd(2)–Cl(1)	84.09(3)
C(1)–Pd(1)–P(4)	90.33(9)	P(3)–Pd(2)–Cl(1)	92.91(3)
P(1)–Pd(1)–Cl(1)	92.21(3)	C(2)–Pd(2)–Cl(1)	175.24(9)
P(4)–Pd(1)–Cl(1)	85.31(3)	P(3)–Pd(2)–P(2)	175.62(3)
C(1)–Pd(1)–Cl(1)	175.01(9)	Pd(1)–Cl(1)–Pd(2)	73.59(2)
P(1)–Pd(1)–P(4)	176.70(3)	P(1)–C(3)–P(2)	114.52(16)
C(2)–Pd(2)–P(2)	91.17(9)	P(3)–C(32)–P(4)	114.04(17)
C(2)–Pd(2)–P(3)	91.80(9)		

plexes $[\text{Pd}_2\text{HMe}(\mu\text{-Cl})(\mu\text{-dppm})_2]\text{BPh}_4$ [3.031(1) Å³⁷], $[\text{Pd}_2\text{-Cl}_2(\mu\text{-Cl})(\mu\text{-dppm})_2]\text{OH}$ [3.170 Å³⁸], and $[\text{Pd}_2\text{Bz}_2(\mu\text{-Br})(\mu\text{-dppm})]\text{PF}_6$ [3.356 Å³⁸] though the electron count suggests the absence of a Pd–Pd bond. The P–Pd \cdots Pd–P torsion angle of 20.9 $^\circ$ reflects a significant degree of twisting around the Pd \cdots Pd axis; a similar twist was observed in $[\text{Pd}_2\text{Bz}_2(\mu\text{-Br})(\mu\text{-dppm})_2]\text{PF}_6$,³⁸ and as in the structure of **5** the likely origin is in the reduction of steric interactions between ligands on the two coordination centers.

Formation of the Ruthenium(II) Dimer $[\text{Ru}_2\text{Cp}^*_2(\mu\text{-Cl})_2(\mu\text{-L})]$. The ruthenium tetramer $[\text{RuCp}^*(\mu_3\text{-Cl})]_4$ generally reacts with phosphines to give either 16-electron complexes $[\text{RuCp}^*\text{ClL}]$ or 18-electron complexes $[\text{RuCp}^*\text{ClL}_2]$. In order to determine whether **L** would coordinate in a monodentate or bidentate mode, 4 equiv of **L** was added to a solution of $[\text{RuCp}^*(\mu_3\text{-Cl})]_4$. NMR spectra showed that only 2 equiv of **L** reacted, leading to formation of the dimer $[\text{Ru}_2\text{Cp}^*_2(\mu\text{-Cl})_2(\mu\text{-L})]$ **8** instead of monomeric complexes.

The $^{31}\text{P}\{^1\text{H}\}$ NMR spectrum of **8** consists of two doublets at δ 119.1 and δ 34.6 with a coupling constant of 24 Hz. The lower field signal can be assigned to the phosphorus atom with pyrrolyl substituents and the higher field signal to the phosphorus atom with phenyl substituents. Both signals are shifted downfield compared with the analogous signals for **L** in agreement with a bridging coordination mode. The ^1H NMR spectrum of **8** contains the expected signals for a dimeric complex with one bridging molecule of **L**. The signals for the protons of the two chemically inequivalent Cp* rings are observed as doublets at δ 1.41 and δ 1.32, both with $^4J_{\text{PH}}$ 2.0 Hz.

Crystals of **8** suitable for a single-crystal X-ray analysis were obtained by slow evaporation of a THF–hexane solution. The analysis confirmed the dimeric nature of **8**, with the molecular structure shown in Figure 8 and selected bond lengths and angles given in Table 6. Each ruthenium center is coordinated to a pentamethylcyclopentadienyl ring, two bridging chlorides, and a bridging **L** ligand. The Ru–P bond to the diphenylphosphino group is longer than that to

(37) Young, S. J.; Kellenberger, B.; Reibenspies, J. H.; Himmel, S. E.; Manning, M.; Anderson, O. P.; Stille, J. K. *J. Am. Chem. Soc.* **1988**, *110*, 5744–5753.

(38) Stockland, R. A., Jr.; Janka, M.; Hoel, G. R.; Rath, N. P.; Anderson, G. K. *Organometallics* **2001**, *20*, 5212–5219.

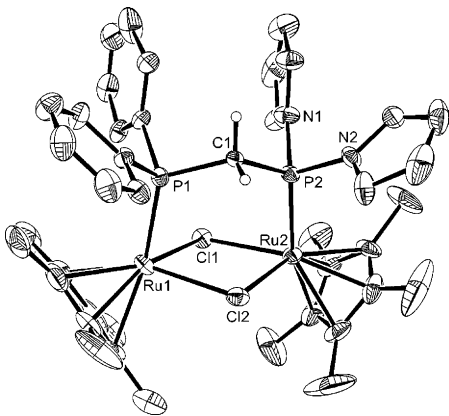


Figure 8. Molecular structure of $[\text{Ru}_2\text{Cp}^*_2(\mu\text{-Cl})_2(\mu\text{-L})]$ **8** with the phenyl, pyrrolyl, and methyl protons omitted for clarity and thermal ellipsoids shown at the 30% probability level.

Table 6. Selected Bond Lengths (Å) and Angles (deg) for Complex **8**

Ru(1)–P(1)	2.2888(19)	Ru(1A)–P(1A)	2.3070(19)
Ru(1)–Cl(1)	2.483(2)	Ru(1A)–Cl(1A)	2.4754(18)
Ru(1)–Cl(2)	2.4763(19)	Ru(1A)–Cl(2A)	2.476(2)
Ru(2)–P(2)	2.2596(17)	Ru(2A)–P(2A)	2.2502(18)
Ru(2)–Cl(1)	2.4635(18)	Ru(2A)–Cl(1A)	2.476(2)
Ru(2)–Cl(2)	2.465(2)	Ru(2A)–Cl(2A)	2.454(2)
P(2)–N(1)	1.737(7)	P(2A)–N(1A)	1.736(7)
P(2)–N(2)	1.790(6)	P(2A)–N(2A)	1.754(6)
P(1)–Ru(1)–Cl(1)	88.72(7)	P(1A)–Ru(1A)–Cl(1A)	89.77(6)
P(1)–Ru(1)–Cl(2)	89.00(6)	P(1A)–Ru(1A)–Cl(2A)	87.70(7)
P(2)–Ru(2)–Cl(1)	90.31(6)	P(2A)–Ru(2A)–Cl(1A)	87.01(7)
P(2)–Ru(2)–Cl(2)	86.90(7)	P(2A)–Ru(2A)–Cl(2A)	91.05(6)
Cl(2)–Ru(1)–Cl(1)	81.20(7)	Cl(1A)–Ru(1A)–Cl(2A)	81.44(7)
Cl(1)–Ru(2)–Cl(2)	81.82(7)	Cl(2A)–Ru(2A)–Cl(1A)	81.88(7)
Ru(2)–Cl(1)–Ru(1)	97.86(7)	Ru(1A)–Cl(1A)–Ru(2A)	97.48(7)
Ru(2)–Cl(2)–Ru(1)	97.99(7)	Ru(2A)–Cl(2A)–Ru(1A)	98.06(7)
C(1)–P(1)–Ru(1)	117.1(2)	C(1A)–P(1A)–Ru(1A)	115.6(2)
C(1)–P(2)–Ru(2)	119.8(2)	C(1A)–P(2A)–Ru(2A)	119.3(2)
P(2)–C(1)–P(1)	119.7(4)	P(2A)–C(1A)–P(1A)	119.7(4)

the di(*N*-pyrrolyl)phosphino group, as anticipated given the electronic difference between the two phosphino groups. The Ru···Ru distance is 3.722 Å, consistent with the absence of a metal–metal bond.

The synthesis of **8** is similar to the reaction of $[\text{RuCp}^*(\mu_3\text{-Cl})_4]$ with dppm, which has been reported to give $[\text{Ru}_2\text{Cp}^*_2(\mu\text{-Cl})_2(\mu\text{-dppm})]$.³⁹ This is in contrast to the reaction of $[\text{RuClCp}^*(\text{cod})]$ with dppm which gives $[\text{RuCp}^*\text{Cl}(\text{dppm})]$.⁴⁰ Additional interest in these reactions derives from the body of thermochemical data that has been reported for ligands such as phosphines,^{22,41–43} phosphites,⁴⁴ and *N*-heterocyclic carbenes,⁴⁵ which has enabled the relative importance of electronic and steric factors to be assessed.

(39) Mauthner, K.; Kalt, D.; Slugovc, C.; Mereiter, K.; Schmid, R.; Kirchner, K. *Monatsh. Chem.* **1997**, *128*, 533–540.

(40) Luo, L.; Zhu, N.; Zhu, N. J.; Stevens, E. D.; Nolan, S. P.; Fagan, P. J. *Organometallics* **1994**, *13*, 669–675.

(41) Luo, L.; Nolan, S. P.; Fagan, P. J. *Organometallics* **1993**, *12*, 4305–4311.

(42) Shen, J. Y.; Stevens, E. D.; Nolan, S. P. *Organometallics* **1998**, *17*, 3000–3005.

(43) Smith, D. C.; Haar, C. M.; Luo, L. B.; Li, C. B.; Cucullu, M. E.; Mahler, C. H.; Nolan, S. P.; Marshall, W. J.; Jones, N. L.; Fagan, P. J. *Organometallics* **1999**, *18*, 2357–2361.

(44) Serron, S. A.; Luo, L. B.; Stevens, E. D.; Nolan, S. P.; Jones, N. L.; Fagan, P. J. *Organometallics* **1996**, *15*, 5209–5215.

(45) Huang, J.; Jafarpour, L.; Hillier, A. C.; Stevens, E. D.; Nolan, S. P. *Organometallics* **2001**, *20*, 2878–2882.

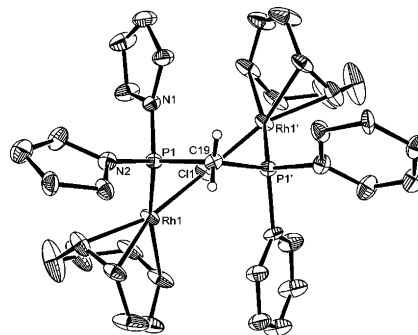


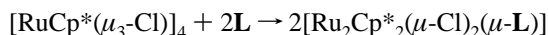
Figure 9. Molecular structure of $[\text{Rh}_2(\mu\text{-Cl})(\text{cod})_2(\mu\text{-L})]\text{PF}_6\cdot\text{CH}_2\text{Cl}_2$ (**9**· CH_2Cl_2) with the phenyl, pyrrolyl, and cyclooctadiene protons, anion, and included solvent omitted for clarity and thermal ellipsoids shown at the 30% probability level.

Table 7. Selected Bond Lengths (Å) and Angles (deg) for Complex **9**· CH_2Cl_2^a

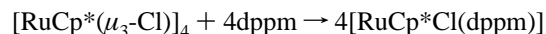
Rh(1)–P(1)	2.2618(9)	Rh(1)–C(15)	2.122(4)
Rh(1)–Cl(1)	2.4074(7)	Rh(1)–C(18)	2.231(4)
Rh(1)–C(11)	2.236(3)	P(1)–N(1)	1.679(8)
Rh(1)–C(14)	2.120(4)	P(1)–N(2)	1.755(5)
P(1)–Rh(1)–Cl(1)	90.31(3)	P(1)–C(19)–P(1')	113.8(3)
Rh(1)–Cl(1)–Rh(1)'	120.78(5)		

^a Primed atoms generated by the symmetry operation $-x + 1, y, -z + 1/2$.

Calorimetric studies indicated that ΔH_{rxn} for the reaction



is $-74.1(2)$ kcal mol⁻¹, whereas the value for the reaction



it is calculated to be $-117.4(2)$ kcal mol⁻¹.⁴⁰ Although the two values are not directly comparable, these initial results suggest that substitution of two phenyl groups by two *N*-pyrrolyl groups markedly decreases ΔH_{rxn} , which is consistent with observations comparing PPh_3 and $\text{P}(\text{NC}_4\text{H}_4)_3$.²²

Formation of the Rhodium(I) Dimer $[\text{Rh}_2(\mu\text{-Cl})(\text{cod})_2(\mu\text{-L})]\text{PF}_6$. The reaction of $[\text{Rh}(\mu\text{-Cl})(\text{cod})_2]$ with **L** was expected to proceed with cleavage of the chloride bridges to give either $[\text{RhCl}(\text{cod})(\text{L}-\kappa^1\text{P})]$ or $[\text{Rh}(\text{cod})(\text{L}-\kappa^2\text{P},\text{P})]^+$. However, the reaction resulted in a mixture from which no product could be isolated. Similar mixtures resulted from the reaction in the presence of NH_4PF_6 , though in this case crystallization by slow diffusion of hexane into a dichloromethane solution gave an orange powder and a small quantity of yellow crystals **9**. Although the powder was revealed to be a mixture, the yellow crystals gave a reasonably simple $^{31}\text{P}\{^1\text{H}\}$ NMR spectrum. This was composed of a doublet of doublets at δ 109.2 with coupling constants of 218 and 72 Hz, and a doublet of doublets at δ 25.8 with coupling constants of 145 and 72 Hz, in addition to the characteristic septet for PF_6^- .

The identity of **9** as $[\text{Rh}_2(\mu\text{-Cl})(\text{cod})_2(\mu\text{-L})]\text{PF}_6$ was confirmed by X-ray crystallography, with the compound crystallizing as **9**· CH_2Cl_2 . The structure of the cation in **9** is shown in Figure 9, and selected bond distances and angle are given in Table 7. The asymmetric unit consists of half a

Table 8. Crystallographic Data for Complexes **2**·CHCl₃, **3**·CH₂Cl₂, **4**, **5**· $\frac{1}{4}$ CH₂Cl₂, **6**, **7**·2CH₂Cl₂, **8** and **9**·CH₂Cl₂

	2 ·CHCl ₃	3 ·CH ₂ Cl ₂	4	5 · $\frac{1}{4}$ CH ₂ Cl ₂	6	7 ·CH ₂ Cl ₂	8	9 ·CH ₂ Cl ₂
empirical formula	C ₂₂ H ₂₁ Cl ₅ -N ₂ P ₂ Pd	C ₂₂ H ₂₂ Cl ₄ -N ₂ P ₂ Pt	C ₄₂ H ₃₆ Cl ₂ -N ₄ P ₄ Pd	C _{42.25} H _{40.50} Cl _{2.50} -N ₄ O ₂ P ₄ Pd ₂	C ₄₄ H ₄₆ Cl ₂ -N ₄ P ₄ Pd ₂	C ₄₆ H ₅₀ Cl ₅ -F ₆ N ₄ P ₅ Pd ₂	C ₄₁ H ₅₀ Cl ₂ -N ₂ P ₂ Ru ₂	C ₃₈ H ₄₂ Cl ₃ -F ₆ N ₂ P ₃ Rh ₂
<i>M</i>	659.00	713.25	897.93	1061.59	1038.42	1317.80	905.81	1045.82
<i>T</i> /K	170(2)	150(2)	150(2)	293(2)	150(2)	150(2)	150(2)	150(2)
λ /Å	0.71073	0.71073	0.71073	0.71073	0.71073	0.71073	0.71073	0.71073
cryst syst	monoclinic	triclinic	triclinic	monoclinic	monoclinic	triclinic	monoclinic	monoclinic
space group	<i>P</i> 2 ₁ / <i>c</i>	<i>P</i> $\bar{1}$	<i>P</i> $\bar{1}$	<i>P</i> 2 ₁ / <i>c</i>	<i>P</i> 2 ₁ / <i>c</i>	<i>P</i> $\bar{1}$	<i>P</i> 2 ₁	<i>C</i> 2/ <i>c</i>
<i>a</i> /Å	10.6090(2)	8.14100(10)	9.3820(2)	13.2580(2)	10.1650(2)	13.3250(3)	17.3300(3)	15.6150(4)
<i>b</i> /Å	17.0690(3)	10.43800(10)	10.5300(2)	15.8300(2)	17.1910(3)	15.1020(3)	12.0900(2)	16.6400(4)
<i>c</i> /Å	14.5520(3)	15.0570(2)	22.6890(4)	21.0940(3)	12.4510(2)	15.1540(3)	20.7670(4)	15.7910(4)
α /deg	90	77.2310(6)	91.1460(10)	90	90	65.136(1)	90	90
β /deg	96.6390(7)	84.1030(6)	99.3950(10)	107.7090(8)	102.2590(8)	83.041(1)	114.132(1)	92.1460(10)
γ /deg	90	86.3170(6)	109.7990(8)	90	90	77.135(1)	90	90
<i>V</i> /Å ³	2617.48(9)	1240.10(3)	2073.85(7)	4217.30(10)	2126.16(7)	2696.08(10)	3970.83(12)	4100.16(18)
<i>Z</i>	4	2	2	4	2	2	4	4
<i>d</i> _{calc} /g cm ⁻³	1.672	1.910	1.438	1.671	1.622	1.623	1.515	1.694
μ /mm ⁻¹	1.356	6.231	0.766	1.205	1.160	1.121	1.007	1.176
<i>R</i> 1, <i>wR</i> 2	0.0564,	0.0238,	0.0448,	0.0474,	0.0305,	0.0628,	0.0508,	0.0407,
[<i>I</i> > 2 σ (<i>I</i>)]	0.1320	0.0583	0.1248	0.1387	0.0718	0.1420	0.1028	0.0938
<i>R</i> indices	0.0594,	0.0256,	0.0664,	0.0720,	0.0423,	0.0882,	0.0945,	0.0743,
(all data)	0.1334	0.0595	0.1416	0.1653	0.0782	0.1598	0.1186	0.1099

dimeric cation, half a PF₆⁻ anion, and half a molecule of dichloromethane. In a manner similar to the structure of **5**, the pyrrolyl and phenyl groups are disordered in a 1:1 ratio. Each rhodium(I) center is in a square planar coordination geometry with an angle of 62° between the two coordination planes. The Rh(1)···Rh(1)' distance at 4.18 Å confirms the absence of a metal–metal bond in agreement with the formal electron count. Due to the disorder in the structure, the Rh–P bond distances appear identical for both phosphorus atoms of **L**, whereas the P–C–P angle of 113.8(3)° is comparable with those observed in the other structures with bridging **L**.

Discussion

The reactions described above demonstrate that **L** can act as a monodentate, chelating, or bridging ligand in a manner similar to dppm. However, there are both structural and reactivity differences between the two ligands, which center on the fact that the di(*N*-pyrrolyl)phosphino group is a poorer σ -donor and better π -acceptor than the diphenylphosphino group. Thus, in the complexes studied, the M–P bonds involving the P(NC₄H₄)₂ groups are shorter, typically by ~0.03 Å, than those to the PPh₂ groups due to the greater π -character. However, the poorer σ -donor capability of the di(*N*-pyrrolyl)phosphino groups means that these bonds are also weaker than the M–PPh₂ bonds, as witnessed by the reaction of [PdCl₂(**L**- κ^2 P,*P'*)] **2** with **L** to give exclusively *trans*-[PdCl₂(**L**- κ^1 P)₂] **4**. This relative weakness of the Pd–P(NC₄H₄)₂ bond leads to a marked difference in the chemistry of **L** with respect to dppm, since [PdCl₂(dppm- κ^2 P,*P*)] reacts with dppm to give [Pd(dppm- κ^2 P,*P*)₂]Cl₂, following displacement of chloride, rather than [PdCl₂(dppm- κ^1 P)₂] following displacement of the phosphino group.^{46,47} Moreover, with dppm complexes, stronger field ligands such as cyanide or acetylides are required to prepare compounds of the type

[PdX₂(dppm- κ^1 P)₂].^{46–48} Such compounds exhibit fluxional behavior in solution, in contrast to **4** for which the ³¹P{¹H} NMR spectra are temperature invariant.

Although the palladium dimers [Pd₂Cl₂(μ -**L**)₂] **5**, [Pd₂Cl₂(CH₃)₂(μ -**L**)₂] **6**, and [Pd₂(CH₃)₂(μ -Cl)(μ -**L**)₂]PF₆ **7** all have dppm analogues, the presence of two unsymmetrical diphosphine ligands affords possibilities of isomerism, and an opportunity to study interconversion between these isomers. The palladium(I) dimer **5** exists both in solution and in the solid state as a 1:1 mixture of HH and HT isomers. In solution, the ratio of the isomers is neither temperature nor concentration dependent, and interconversion of the isomers was not observed on the NMR time scale. In contrast, the HH and HT isomers of **6** do interconvert in solution, and the position of equilibrium in this instance is temperature dependent. At low temperatures the HT isomer is dominant and is isolable by crystallization. The formation of both HH and HT isomers of **6** is similar to previous observations on the reaction of [PdCl(CH₃)(cod)] with the arsino(phosphino)methane Pr₂AsCH₂PPr₂, though reaction with the bulkier ligand Bu₂AsCH₂PPr₂ gave the chelate complex [PdCl(CH₃)(Bu₂AsCH₂PPr₂- κ^2 P,*As*)] rather than a dimer.⁸ The A-frame dimer **7** exists as both HH and HT isomers in solution, with the HT complex dominant in the original reaction mixture. These isomers do not interconvert in solution, and the HT isomer can be isolated by fractional crystallization.

Formation of **9** from the reaction between [Rh(μ -Cl)(cod)]₂ and **L** in the presence of NH₄PF₆, albeit in low yield, contrasts with similar reactions involving dppm or arsino(phosphino)methanes. The reaction of [Rh(μ -Cl)(nbd)]₂ (nbd = norbornadiene) with dppm gave a mixture of [Rh(dppm- κ^2 P,*P*)₂]⁺ and [Rh(nbd)(dppm- κ^2 P,*P*)]⁺,⁴⁹ whereas the reaction of [Rh(μ -Cl)(cod)]₂ with a range of arsino(phosphino)methanes in the presence of KPF₆ gave [Rh(cod)(PR₂CH₂-

(46) Pringle, P. G.; Shaw, B. L. *J. Chem. Soc., Chem. Commun.* **1982**, 956.

(47) Hassan, F. S. M.; Markham, D. P.; Pringle, P. G.; Shaw, B. L. *J. Chem. Soc., Dalton Trans.* **1985**, 279.

(48) Langrick, C. R.; Pringle, P. G.; Shaw, B. L. *Inorg. Chim. Acta* **1983**, 76, L263.

(49) Ernsting, J. M.; Elsevier, C. J.; de Lange, W. G.; Timmer, K. *Magn. Reson. Chem.* **1991**, 29, S118–S124.

AsR₂-κ²P,As)]PF₆. However, in the absence of KPF₆ the product depended on the steric bulk of the substituents.⁷

In addition to influencing the course of the reaction, alteration of the steric demands within one of the phosphino groups in **L** would be expected to reduce the potential for the phenyl/pyrrolyl disorder that was observed in the crystal structures of **5** and **9**. Thus future work will focus on the development of ligands in which the isostericity is lifted and, in addition, the electronic difference between the two donor groups is further exaggerated.

Acknowledgment. The authors would like to thank the EPSRC for financial support, the Royal Society of Chemistry for a journal grant for international authors (to A.D.B.) and Johnson-Matthey plc for a generous loan of platinum metals.

Supporting Information Available: X-ray crystallographic data in CIF format. This material is available free of charge via the Internet at <http://pubs.acs.org>.

IC034487Z